Modeling for Primary Radical Desorption in Miniemulsion Polymerization Initiated by Oil-Soluble Initiator

Yue Shang, Guorong Shan, and Pengju Pan
State Key Laboratory of Chemical Engineering, Dept. of Chemical and Biological Engineering, Zhejiang University, Hangzhou 310027, China

DOI 10.1002/aic.14506
Published online June 2, 2014 in Wiley Online Library (wileyonlinelibrary.com)

Primary radical (PR) desorption in the miniemulsion polymerization initiated by oil-soluble initiator was investigated. Both the aqueous phase inhibition experiments and the theoretical predictions, which combined the two film theory and aqueous phase mass balance, were performed to evaluate the PR desorption process quantitatively. The theoretical predictions agreed well with the experiment results. It was found that the organic phase diffusion, particle size, surfactant layer, aqueous phase resistance, and different initiator type affected the PR desorption. The desorption rate of PR was faster than its reaction rate at the early stage of polymerization, while the former decreased to a comparable level as the latter at the high conversion. PR was prone to desorb in the polymerization and the desorption of PR played a critical role in the miniemulsion polymerization initiated by oil-soluble initiator. It is concluded that the PR desorption–reabsorption is a process to generate effective radicals in the miniemulsion polymerization initiated by oil-soluble initiator. © 2014 American Institute of Chemical Engineers *AIChE J*, 60: 3276–3285, 2014
Keywords: primary radical, desorption, miniemulsion polymerization, oil-soluble initiator

Introduction

Miniemulsion polymerization has been a feasible *in situ* technic to produce the functional colloid particles with well-defined architectures. Such particles may have core-shell structures,[1–3] functional surface,[4,5] or environmental sensitivity.[6] For synthesizing such particles, different initiators are always used to obtain the desired morphology, function, and polymerization rate.[1,2,4,5,7] In some cases, only the water-soluble or oil-soluble initiator is suitable to synthesize the materials with specified structures, because the source of radical is different.[2]

When the water-soluble initiator is used, the polymerization is similar to the conventional emulsion system, where the ionic primary radical (PR) propagates in the aqueous phase to a critical chain length to become a surface active oligomer radical. The surface active oligomer radical will be absorbed by the submicron droplets.[8] However, when oil-soluble initiator is used in miniemulsion polymerization, the polymerization will become quite complicated. In this case, the initiator is enriched in the submicron droplets and decomposes in such a compartmentalized space. According to the classic theory, the two radicals that exist within a small particle will suffer rapid mutual termination instantaneously and the polymerization cannot proceed.[9] However, the oil-soluble initiators are frequently used in miniemulsion polymerization and the polymerization can proceed well. Therefore, the origin of effective radicals is a critical factor determining the kinetics of miniemulsion polymerization initiated by oil-soluble initiator. Although some authors have claimed that the effective radicals come from the decomposition of small amount of oil-soluble initiator dissolved in the aqueous phase,[10–12] other authors claimed that the radicals desorbed from particle played important roles.[13–16] This debate has lasted for quite a long time and remained unsolved.

The radical desorption is common in emulsion polymerization, especially in the system where the monomer of high water solubility is used.[17] Much effort has been exerted to investigate the radical desorption experimentally and theoretically.[18–25] In the PR desorption models published in the literatures, the partition coefficient of initiator is always used.[10,11,26] However, it has been reported that the partition coefficient of PR should be used in the modeling of miniemulsion polymerization initiated by oil-soluble initiator, because PR is more directly related to the polymerization than the initiator.[27] Recently, Hernandez and Tauer have reviewed a range of models to estimate the radical desorption rate in emulsion polymerization.[28,29] Among these models, the expression "Desorption rate $= \frac{\text{Driving force}}{\text{Resistance}}$," was always used, but the assumptions of resistance terms were different.

One direct way to explore the origin of effective radicals formation is to decide the PR desorption rate and compare the desorption rate with its reaction rate. If the PR desorption rate is high enough, the two PRs would desorb from the particle into the aqueous phase without suffering rapid mutual termination. In this case, the desorption of PR is for the origin of effective radicals. If the PR desorption rate is low, the initiator dissolved in the aqueous phase will be the major source for the effective radicals. In this article, we established a novel PR desorption model to clarify the proportion of PR desorbed

Additional Supporting Information may be found in the online version of this article.

Correspondence concerning this article should be addressed to G. R. Shan at shangr@zju.edu.cn.

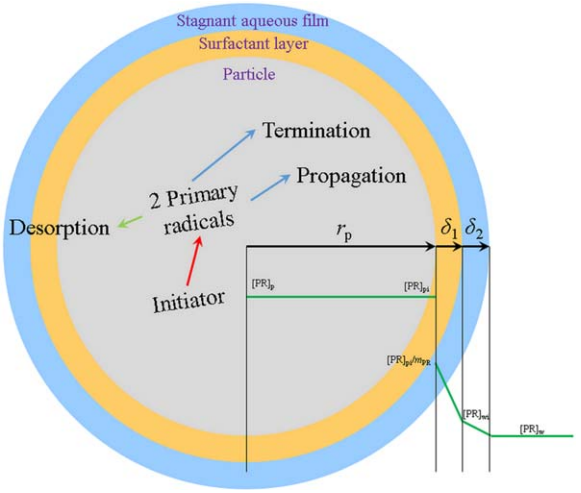

Figure 1. Schematic illustration of PR desorption process.

[Color figure can be viewed in the online issue, which is available at wileyonlinelibrary.com.]

from the particle by considering both the desorption and reaction rates of PR quantitatively. A lot of variables such as the diffusion coefficient of PR, particle size, and partition coefficient of PR were included and reliable assumptions and parameters were applied in modeling. A new experiment procedure for evaluating the radical desorption rate was also proposed to compare with the model predictions. This method can measure the desorption rate directly. The origin of effective radicals was discussed based on the model predictions and experiment results.

PR Desorption Model

In this work, a PR desorption model was proposed to illustrate the behavior of PR in miniemulsion polymerization initiated by oil-soluble initiator. This model of PR desorption is originated from the two film theory, which is based on the mass-transfer driving force between the two sides of film. The universal expression in each film is

$$R_d = k \cdot a \cdot \Delta[PR] \tag{1}$$

where R_d is the desorption rate, k is the desorption rate coefficient, a is the average surface area of film, and $\Delta[PR]$ is the driving force of mass transfer.

The desorption process is illustrated in Figure 1 in detail, which can be divided into three parts, including the mass transfers in the particle, surfactant layer, and the stagnant aqueous film surrounding the particle.

The mass-transfer rates in the particle (R_p), the surfactant layer around the particle (R_{sl}), and the stagnant aqueous film outside the surfactant layer (R_w) are expressed as

$$R_p = 4\pi r_p^2 k_{mt} \left([PR]_p - [PR]_{pi} \right) N_A \tag{2}$$

$$R_{sl} = 4\pi r_p \frac{(r_p + \delta_1)}{\delta_1} D_{sl} \left(\frac{[PR]_{pi}}{m_{PR}} - [PR]_{wi} \right) N_A \tag{3}$$

$$R_w = 4\pi (r_p + \delta_1) \frac{(r_p + \delta_1 + \delta_2)}{\delta_2} D_w \left([PR]_{wi} - [PR]_w \right) N_A \tag{4}$$

where r_p is the radius of particle, k_{mt} is the desorption rate coefficient in particle, δ_1 is the thickness of surfactant layer, δ_2 is the thickness of stagnant aqueous film, D_{sl} and D_w are the diffusion coefficients of PR in the surfactant layer and stagnant aqueous film, respectively, N_A is the Avogadro's constant, m_{PR} is the partition coefficient of PR between the miniemulsion droplet (and particle) and water, $[PR]_p$ is the concentration of PR in the particle, $[PR]_{pi}$ is the concentration of PR at the boundary between particle and surfactant layer, $[PR]_{wi}$ is the concentration of PR at the boundary between surfactant layer and stagnant aqueous film, $[PR]_w$ is the concentration of PR in the aqueous phase. According to Einstein diffusion equation,[30] k_{mt} can be expressed as[20]

$$k_{mt} = D_p / 6 r_p \tag{5}$$

where D_p is the diffusion coefficient of PR in the particle.

To simplify this model, two assumptions were made. First, it was assumed that $R_p = R_{sl} = R_w$ under steady conditions. Second, it was assumed that $r_p >> \delta_1$, and $r_p >> \delta_2$, therefore, $r_p + \delta_1 \approx r_p$ and $r_p + \delta_1 + \delta_2 \approx r_p$.

Based on Eqs. 2–5, the desorption rate could be simplified as

$$R_d = \frac{4\pi r_p^2 N_A}{\frac{m_{PR}\,\delta_1}{D_{sl}} + \frac{m_{PR}\,\delta_2}{D_w} + \frac{6 r_p}{D_p}} \left([PR]_p - m_{PR} [PR]_w \right) \tag{6}$$

After the decomposition of initiator, $[PR]_p$ is in the order of 10^{-6} mol/L, which is much larger than $[PR]_w$ (10^{-9} mol/L). Besides, m_{PR} is in the order of 10^1. Therefore, the net desorption rate can be approximated as

$$R_d = \frac{4\pi r_p^2 N_A}{\frac{m_{PR}\,\delta_1}{D_{sl}} + \frac{m_{PR}\,\delta_2}{D_w} + \frac{6 r_p}{D_p}} [PR]_p \tag{7}$$

This model combines as much as factors that may affect the miniemulsion polymerization, which confers this model a wide scope of application.

In Eq. 7, the desorption process of PR was exclusively considered. However, not all of the PRs can escape from the particle, both the desorption and reaction of PR can affect the possibility of PR desorption (P_d) and the origin of effective radicals. Therefore, P_d can be expressed as

$$P_d = \frac{R_d}{R_d + 2 k_{pPR} [M] + k_{tPR} \frac{2}{v_p N_A}} \tag{8}$$

where k_{pPR} is the reaction rate coefficient between PR and monomer, [M] is the monomer concentration in the particle, k_{tPR} is the mutual termination rate coefficient of the PRs, and v_p is the volume of particle.

Experimental Section

Materials

Styrene (St, Sinopharm Chemical Reagent Co.) was washed with 10% aqueous NaOH solution and water to remove the phenol inhibitor, followed by drying over $CaCl_2$ for 24 h. It was further purified by distillation under the reduced pressure. Nitrosyl disulfonate free-radical anion (Fremy's salt, FS) was prepared and purified according to a published method.[31] 2,2′-Azobis(isobutyronitrile) (AIBN, J&K Scientific) was recrystallized twice from ethanol. 2,2′-azobis(2,4-dimethylvaleronitrile) (ABVN, J&K Scientific), 2,2′-azobis(2-methylpropionamide) dihydrochloride (AIBA, J&K Scientific), sodium dodecyl sulfate (SDS, J&K Scientific), Tween-20, hexadecane (Acros Organics) were used as received. Other reagents were purchased from Sinopharm Chemical Reagent Co., and used without further purification. Self-made distilled water was used in all experiments.

Table 1. Recipes for Miniemulsion Prepolymerization Initiated by Oil-Soluble Initiator

	Oil Phase (g)				Aqueous Phase (g)					
Run	St	HD	AIBN	ABVN	H_2O	$NaHCO_3$	SDS	Tween-20	d_p (nm)	PDI[a]
1	90	3.6	0.364	–	510	0.6	1.632	–	85.0	1.05
2	90	3.6	1.092	–	510	0.6	1.632	–	79.8	1.04
3	90	3.6	0.364	–	510	0.6	8.160	–	64.6	1.02
4	90	3.6	0.364	–	510	0.6	–	8.000	115.8	1.01
5	90	3.6	–	0.0765	510	0.6	1.632	–	85.7	1.04
6	90	3.6	0.364	–	510	0.6	0.1632	–	220.0	1.07

[a]PDI is defined as volume average diameter (d_p) over number average diameter.

Miniemulsion polymerization in the presence of FS

The miniemulsion polymerization process was divided into two steps, that is, prepolymerization and postpolymerization. In Step 1, the costabilizer and initiator were predissolved in monomer to form the oil phase. Surfactant and pH buffer were added into water to form the aqueous phase. The oil and aqueous phases were then mixed and the mixture was pre-emulsified under vigorous magnetic agitation for 10 min. The mixture was then homogenized to form the miniemulsion by ultrasonicating for 60 min, which was performed using a pulsed sequence (10 s sonication followed by 5 s break) with a 560 W duty cycle under the magnetic agitation in an ice bath. The miniemulsion was introduced into a jacketed reactor and purged with nitrogen for 25 min at room temperature to remove the oxygen. Then, the temperature was increased to 60°C and maintained at this temperature for the prepolymerization. At specific time intervals, samples were withdrawn with syringe and immediately cooled in an ice bath for the postpolymerization. The recipes of prepolymerization are shown in Table 1.

In Step 2, FS (10 mg FS/100 g sample) was added into the sample withdrawn in the prepolymerization process. The mixture was injected into a jacketed reactor and purged with nitrogen for 25 min to remove the oxygen. Then, the reactant was increased to 60°C and maintained at this temperature for the postpolymerization. Samples of postpolymerization were withdrawn with the same methods at specific time intervals to estimate the polymerization rate.

Confirmation of FS inhibition efficiency

FS and different amount of AIBA were dissolved in 1 wt % $NaHCO_3$ buffered solution. The color fading of the solutions was monitored by a UV-Vis spectrophotometer (UV-1800, SHIMADZU, Japan) at 60°C to decide the decomposition rate coefficient and inhibition efficiency of FS. The maximum absorption wavelength of FS solution is 543.0 nm.

Characterization

The conversions of different samples taken from the postpolymerization were determined gravimetrically. The particle size was estimated by a JEOL JEM-1200EX transmission electron microscope (TEM) operated at 80 kV in which more than 500 particles were counted. Typically, the final samples of each run in prepolymerization were diluted and mounted on the copper grids coated with carbon before TEM analysis.

Results and Discussion

Measurement of PR desorption rate

FS is a kind of nitroxide stable radical, which is only dissolved in the aqueous phase and can efficiently inhibit the radical with carbon center.[31–35] When the desorbed radical is inhibited by FS in the aqueous phase, the polymerization kinetics will be changed. Figure 2 shows the conversion vs. postpolymerization time plot for the samples prepolymerized with different times in Run 1. In the presence of FS, all the samples showed an obvious induction period. This indicated that the radicals in the aqueous phase played important roles in the miniemulsion polymerization initiated by oil-soluble initiator. The radicals in the aqueous phase are originated from the radicals desorption from the particle and the decomposition of initiators dissolved in aqueous phase. However, because the amount of initiator distributed in the aqueous phase is quite small,[10] the decomposition of initiator dissolved in the aqueous phase may not be the major source for the radical in aqueous phase.[26] Therefore, the radicals desorbed from the miniemulsion droplets will be the major source of aqueous phase radicals, which mainly initiate the polymerization. When the diffusion of radicals from the aqueous phase to particle is "switched off" by FS, the polymerization will stop. After FS is completely consumed by the radicals desorbed from the particle, the polymerization restarts. Therefore, the length of induction period is an indicator for the radical desorption rate. Meanwhile, FS inhibits carbon-centered radical stoichiometrically and the change of FS amount in the aqueous phase with polymerization time can be determined by the mass balance of radicals in the aqueous phase and the radical desorption rate calculated by the proposed model. Then, the length of induction period can be obtained theoretically, which can be compared with that derived from experiment to access the reliability of proposed model.

Because FS decomposes on heating,[36] the quantities of FS that undergoes self-decomposition and reacts with the PRs should be clarified. Meanwhile, the initiator decomposes continuously in polymerization. Hence, according to the law of mass action, the mass balance of radicals in aqueous phase can be stated as below

$$\frac{d[PR]}{dt} = 2fk_d[I]P_d - k_{tFS}[PR][FS] - k_{tPR}[PR]^2 \quad (9)$$

$$\frac{d[FS]}{dt} = -k_{dFS}[FS] - k_{tFS}[PR][FS] \quad (10)$$

$$\frac{d[I]}{dt} = -k_d[I] \quad (11)$$

where f is the efficiency of initiation, k_d is the first-order decomposition rate coefficient of initiator, k_{dFS} is the first-order decomposition rate coefficient of FS, k_{tFS} is the reaction rate coefficient between FS and PR, k_{tPR} is the mutual termination rate of PR, P_d can be predicted by the PR desorption model (Eq. 8), [PR] and [FS] are the concentrations of PR and FS in the aqueous phase, respectively, and [I] is the concentration of initiator in the particle.

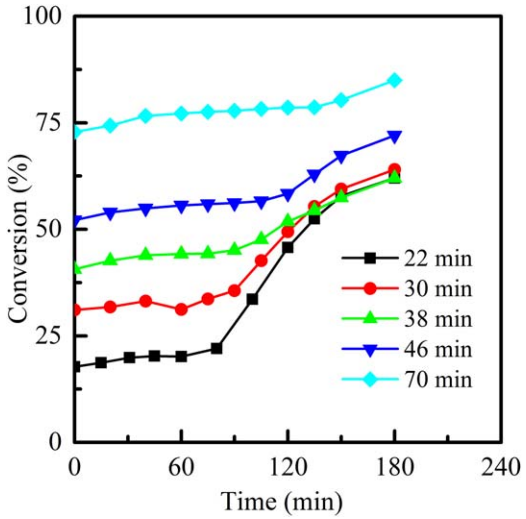

Figure 2. Postpolymerization rate for the samples prepolymerized with different times in Run 1.

[Color figure can be viewed in the online issue, which is available at wileyonlinelibrary.com.]

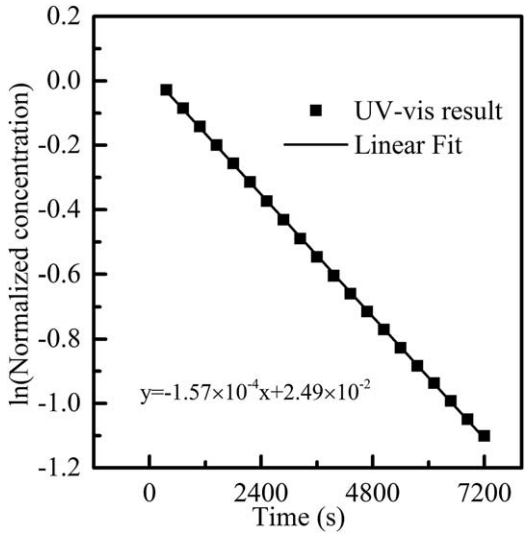

Figure 3. Decomposition rate of FS.

In modeling, P_d was first calculated (Eqs. 7 and 8) and was then substituted into the ordinary differential equations (Eqs. 9–11). The ordinary differential equations were solved numerically to find out the induction period, which equals to the time when the concentration of FS decreased to zero in the aqueous phase.

FS inhibition efficiency

Decomposition of FS obeys the rule of first-order reaction. Figure 3 shows the decomposition rate of FS and its linear fit. As shown in Figure 3, k_{dFS} is 1.57×10^{-4}/s at 60°C. The efficiency of FS and reliability of Eqs. 9–11 can be measured by monitoring the color fading of FS aqueous solution with AIBA as the radical source. Figure 4 compared the experiment results and the results predicted from Eqs. 9–11 with $P_d = 1$. As shown in Figure 4, Eqs. 9–11 can predicate the experiment results well. This confirms the reliability of Eqs. 9–11 and high inhibition efficiency of FS.

Effects of organic phase diffusion coefficient on the possibility of PR desorption

The viscosity of organic particle increases during the polymerization process, which can affect the diffusion rate of PR in three possible ways. First, the diffusion of PR in the particle will become more difficult, resulting in the decrease of PR diffusion rate by several orders of magnitude. This will increase the reaction possibility of PR with the other PR or the monomer inside the particle. Second, as the polymerization progresses, the mutual termination rate will decrease due to the gel effect. The reaction rate between radical and monomer is also reduced, due to the decrease of monomer concentration. Third, the partition coefficient of PR decreases with the increase of conversion, which improves the driving force of desorption. Consequently, besides the organic phase diffusion coefficient, the possibility of PR desorption is also influenced by other factors including the reaction rate and the driving force of desorption.

Because some parameters cannot be measured experimentally, the approximation was made to estimate the parameters (Appendices A and B). The following parameters were used in the prediction: $D_p = 1 \times 10^{-9}$ to 3.8×10^{-7} dm^2/s, $D_{sl} = 1.0 \times 10^{-7}$ dm^2/s, $\delta_1 = 2$ nm, $D_w = 2.5 \times 10^{-7}$ dm^2/s, $\delta_2 = 0$ nm (see below), $m_{PR} = 10.98$–4.34, and $d_p = 85.0$ nm.

For the prepolymerization Run 1 and 2 samples, the induction periods of postpolymerization in the presence of FS are plotted as a function of the initial conversion in Figure 5. As shown in Figure 5, the model predictions agree well with experiment results and the induction period increases with the increase of initial conversion. Figure 6 shows the influences of organic phase diffusion coefficient on the possibility of PR desorption. The possibility of PR desorption decreases with the decrease of organic phase diffusion coefficient. As predicted by this model, the PR originating from the AIBN decomposition can be easily desorbed into the aqueous phase, even though the diffusion coefficient is two orders of magnitude smaller than its initial value. The relatively high possibility of PR desorption can be

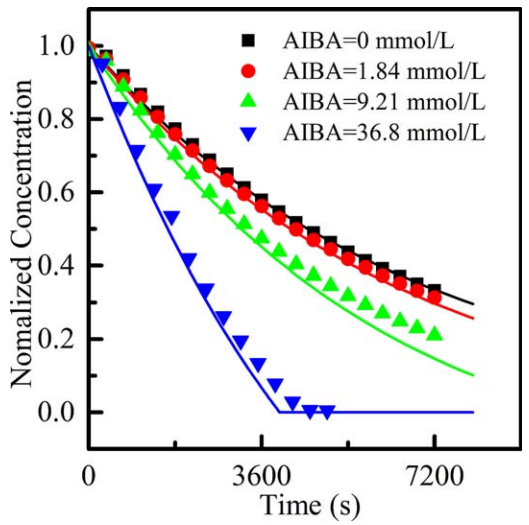

Figure 4. Comparison between experiment results and the results predicted from Eqs. 9 to 11.

The experiment and predicted results are represented by the scatters and solid lines, respectively. [Color figure can be viewed in the online issue, which is available at wileyonlinelibrary.com.]

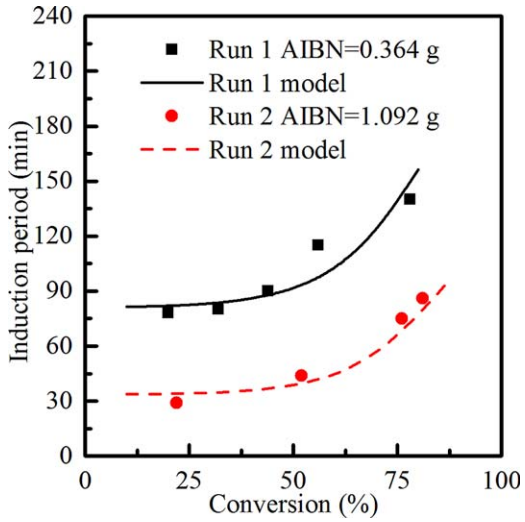

Figure 5. Comparison for the induction periods derived experimentally and predicted from model at different initial conversion.

[Color figure can be viewed in the online issue, which is available at wileyonlinelibrary.com.]

attributable to the hydrophilic nature of PR, as demonstrated by the PR partition coefficient of 10.98–4.34,[27] and the small particle size (85 nm) of miniemulsion system. Such a possibility of PR desorption leads to the relative high rate of miniemulsion polymerization. Otherwise, if the PRs do not desorb from the particle, they will suffer rapid mutual termination, leading to the dramatic decrease of polymerization rate.

Effects of particle size on the possibility of PR desorption

As a critical variable in the miniemulsion polymerization, the particle size is usually a key factor for the PR desorption and polymerization. To investigate the effects of particle size on the possibility of PR desorption, the samples of prepolymerized miniemulsion (Runs 1, 3, and 6) with different particle sizes were used in the postpolymerization in the presence

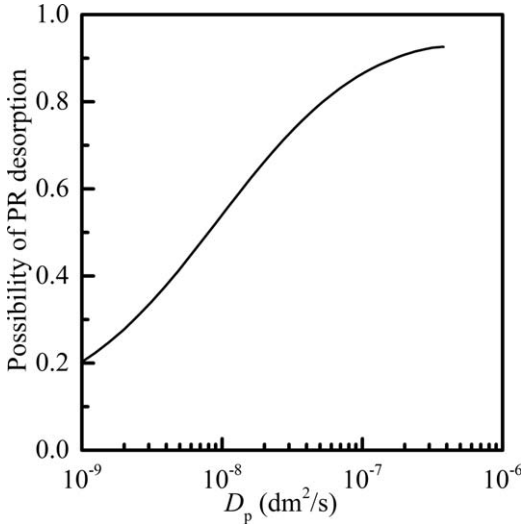

Figure 6. Theoretically predicted relationship between organic phase diffusion coefficient (D_p) and possibility of PR desorption (P_d).

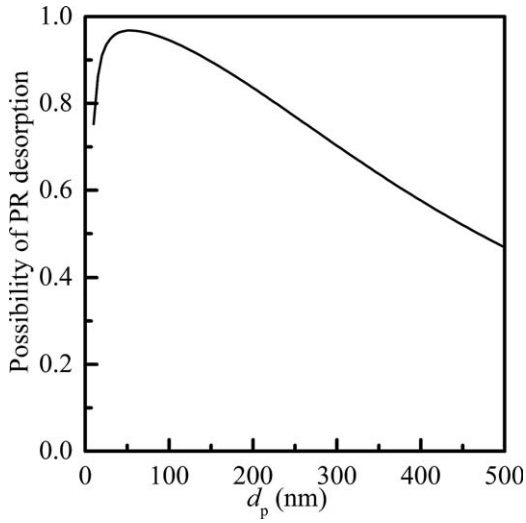

Figure 7. Theoretically predicted relationship between particle size (d_p) and possibility of PR desorption (P_d).

of FS. The following parameters were used in the prediction: $D_p = 3.8 \times 10^{-7}$ dm^2/s, $D_{sl} = 1.0 \times 10^{-7}$ dm^2/s, $\delta_1 = 2$ nm, $D_w = 2.5 \times 10^{-7}$ dm^2/s, $\delta_2 = 0$ nm, $m_{PR} = 10.98$, and $d_p = 10$–200 nm.

Generally, the mutual termination is rapid and the desorption of PR is less obvious in the smaller particles. According to the model analysis in Figure 7, this phenomenon only occurs when the particle diameter is smaller than 40 nm. As shown in Figure 7, when the particle size is larger than 40 nm, the possibility of PR desorption decreases with the increase of particle size. That is because the desorption rate is inversely proportional to the surface area of particle, the termination rate is inversely proportional to the volume of the particle, and the propagation rate is constant (Eqs. 7 and 8). In the particle size range of common miniemulsion polymerization, the PR desorption is significant and thus is the main origin of effective radicals. Figure 8 shows the comparison of model predictions and experiments results at different particle sizes. As shown in this figure, when the particles are small (64.6 and 85.0 nm), the particle size does not have noticeable effect on the induction period of postpolymerization. When the particles are large (220.0 nm), the induction time is longer than the case with small particles. These experiment results agree with model predictions, because the systems with particle sizes of 64.6 and 85.0 nm have the similar possibility of PR desorption, and the possibility of PR desorption decreases with the further increase of particle size (Figure 7).

Effects of surfactant layer property on the possibility of PR desorption

In the miniemulsion polymerization, the surfactant is adsorbed on the surface of latex and prevents the coagulation of colloid particles. Depending on the chemical structure of surfactant, the surfactant layer may be much different, which will affect the PR desorption. In the modeling, the surfactant layer was treated as a film having a defined thickness and diffusion resistance. The following parameters were used in the prediction: $D_p = 3.8 \times 10^{-7}$ dm^2/s, $D_{sl} = 1.0 \times 10^{-7}$ to 1×10^{-10} dm^2/s, $\delta_1 = 0$–19 nm, $D_w = 2.5 \times 10^{-7}$ dm^2/s, $\delta_2 = 0$ nm, $m_{PR} = 10.98$, and $d_p = 85.0$ nm.

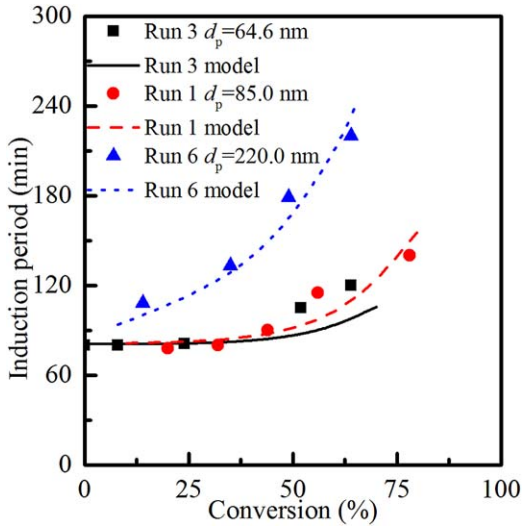

Figure 8. Comparison for the induction periods derived experimentally and predicted from model with particle of different sizes.

[Color figure can be viewed in the online issue, which is available at wileyonlinelibrary.com.]

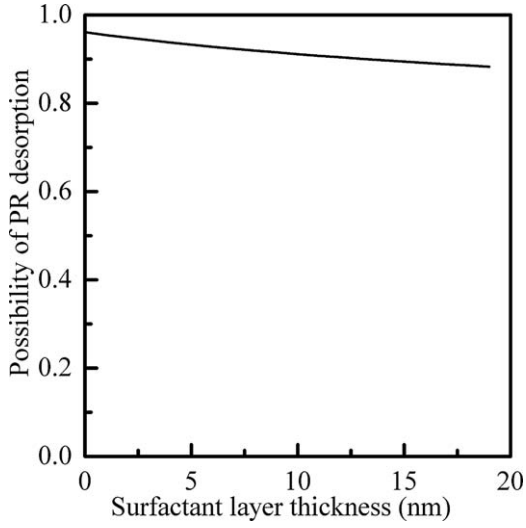

Figure 10. Theoretically predicted relationship between surfactant layer thickness (δ_1) and possibility of PR desorption (P_d) at $D_{sl} = 1.0 \times 10^{-7}$ dm^2/s.

Figure 9 shows the effect of surface layer on the possibility of PR desorption. As shown in Figure 9, the diffusion coefficient in the surfactant layer has a significant effect on the possibility of PR desorption. As the diffusion coefficient in the surfactant layer decreases from 1×10^{-7} to 1×10^{-10} dm^2/s, the possibility of PR desorption decrease from about 95% to below 10%. This model covers the diffusion coefficient in the surfactant layer within a wide range. Therefore, it is considered that this model is suitable to the miniemulsion polymerization with different kinds of surfactants.

Figure 10 shows the theoretical relationship between the thickness of surfactant layer and the possibility of PR desorption at $D_{sl} = 1.0 \times 10^{-7}$ dm^2/s predicted from the model. When the thickness of surfactant layer increases to a large value, the assumption that $\delta_1 << r_p$ is not applicable, and Eq. 7 should be rededuced by simplifying Eqs. 2–4 without any assumptions. In this case, the desorption rate can be expressed as

$$R_d = \frac{4\pi N_A}{\frac{m_{PR}\,\delta_1}{r_p(r_p+\delta_1)D_{sl}} + \frac{m_{PR}\,\delta_2}{(r_p+\delta_1)(r_p+\delta_1+\delta_2)D_w} + \frac{6}{r_p D_p}}[PR]_p \quad (12)$$

With the thickness of surfactant layer increases from 0 to 19 nm, the possibility of PR desorption decreases from about 95% to about 88%, according to Eqs. 12 and 8. This indicates that the effect of surfactant layer thickness on the possibility of PR desorption is rather small. In practical miniemulsion polymerization system, δ_1 is much smaller than r_p.[37,38] Therefore, Eq. 7 is applicable to most of the polymerization systems.

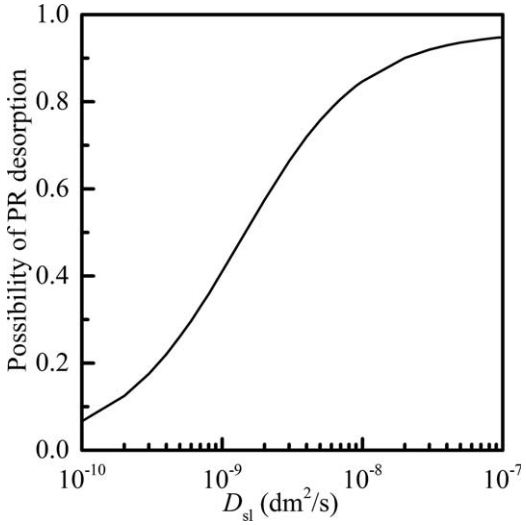

Figure 9. Theoretically predicted relationship between diffusion coefficient in surfactant layer (D_{sl}) and possibility of PR desorption (P_d) at $\delta_1 = 2$ nm.

Figure 11 shows the comparison between model predictions and postpolymerization results with Tween-20 as surfactant, in which the postpolymerization results with SDS as surfactant is also included for comparison. As shown in Figure 11, the predicted induction periods of Run 4 are consistent with the experiment values. Both the predicted and experiment results of Run 4 are larger than those of Run 1. Tween-20 is a nonionic surfactant with polyethylene glycol (PEG) segments, which can form a PEG steric layer after swelling. It has been reported that the diffusion coefficient in PEG is 7.2×10^{-9} dm^2/s,[39] which is much smaller than the diffusion coefficient in SDS layer. The thicknesses of SDS and Tween-20 layers are similar.[37,38] Because the particle size and the thickness of surfactant layer have little effect on the possibility of PR desorption, it is concluded that the diffusion coefficient of PR in the surfactant layer plays an important role in the desorption of PR.

Effects of stagnant aqueous film property on the possibility of PR desorption

Besides the diffusivity of PR in the organic phase and surfactant layer, the diffusivity of PR in the aqueous stagnant film surrounding the particle may affect the possibility of PR desorption. The predicted results illustrating the influences of

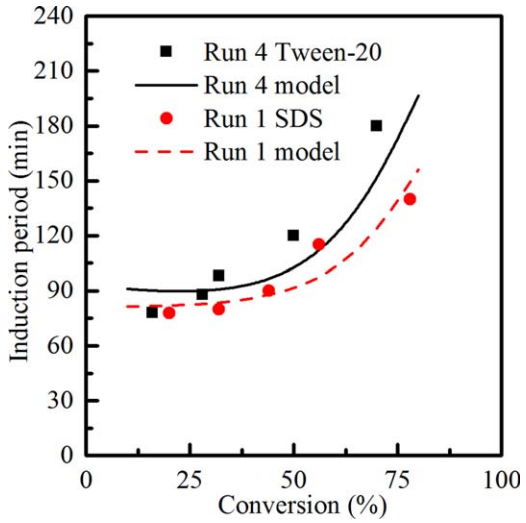

Figure 11. Comparison for the induction periods derived experimentally and predicted from model with Tween-20 and SDS as surfactant.

[Color figure can be viewed in the online issue, which is available at wileyonlinelibrary.com.]

PR diffusion coefficient and thickness of the stagnant aqueous film are shown in Figures 12 and 13. The following parameters were used in the prediction: $D_p = 3.8 \times 10^{-7}$ dm^2/s, $D_{sl} = 1 \times 10^{-7}$ dm^2/s, $\delta_1 = 2$ nm, $D_w = 1 \times 10^{-6}$ to 1×10^{-8} dm^2/s, $\delta_2 = 0$–$0.32d_p$, $m_{PR} = 10.98$, and $d_p = 85.0$ nm.

As shown in Figure 12, the possibility of PR desorption decreases with the decrease of diffusion coefficient in the stagnant aqueous film, according to Eqs.12 and 8. However, in the practical miniemulsion polymerization systems, the diffusivity of PR in the aqueous phase is nearly a constant, because the aqueous phase is mainly made up of water. Therefore, the effect of PR diffusion coefficient can be ignored.

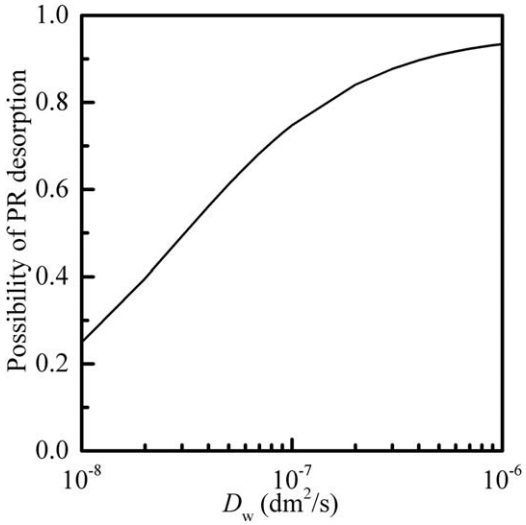

Figure 12. Theoretically predicted relationship between diffusion coefficient in stagnant aqueous film (D_w) and the possibility of PR desorption (P_d) at $\delta_2 = 0.32d_p$.

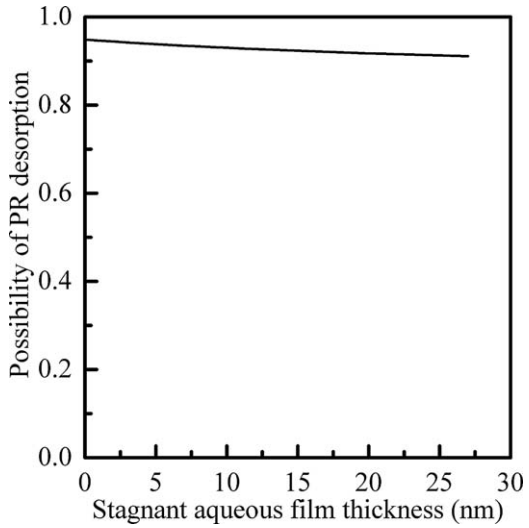

Figure 13. Theoretically predicted relationship between the thickness of stagnant aqueous film (δ_2) and the possibility of PR desorption (P_d) at $D_w = 2.5 \times 10^{-7}$ dm^2/s.

In the experiments, the solid content is 15%. It can be calculated that the average distance between the center of each particle is about $1.65d_p$ (Appendix C), which means that the maximum thickness of stagnant aqueous film is $0.32d_p$. In the existing model published in literature,[26] it has been considered that $r_p << \delta_2$. When the partition coefficient of PR is small, the difference between the model published in Ref. 26 and our model (Eqs. 8 and 12) is minor. However, when the partition coefficient is large, the difference between these two models is obvious (Supporting Information Figure S2), because the smaller diffusion resistance of PR in the stagnant aqueous film is used in our model. Conversely, the model proposed here can also predict the effect of stagnant aqueous film, because the item about stagnant aqueous film was included in modeling. This offers the proposed model more adaptability.

Figure 13 shows the effect of stagnant film thickness, according to Eqs. 12 and 8. It can be seen that the effect of stagnant film thickness is not pronounced. As compared to the formation rate of PR in the particle, the desorption rate of PR and its inhibition rate by FS is dramatically fast, indicating that there is enough time for FS to diffuse to the particle surface. Therefore, the radical diffusion in stagnant aqueous film could be ignored and δ_2 was set to zero in modeling. In this case, it is difficult to evaluate the effect of stagnant aqueous film on the PR desorption rate experimentally. When the diffusions in the particle and surfactant layer are not the rate-determining steps, the stagnant aqueous film will play an important role in the desorption of PR, as described in the next section.

Effect of PR partition coefficient on the possibility of PR desorption

The partition coefficient of PR has great effect on the kinetics of miniemulsion polymerization initiated by oil-soluble initiator.[27] When the different oil-soluble initiators are used in miniemulsion polymerization, the partition coefficient of PR may be different. Therefore, it is necessary to investigate the influence of PR partition on the possibility of

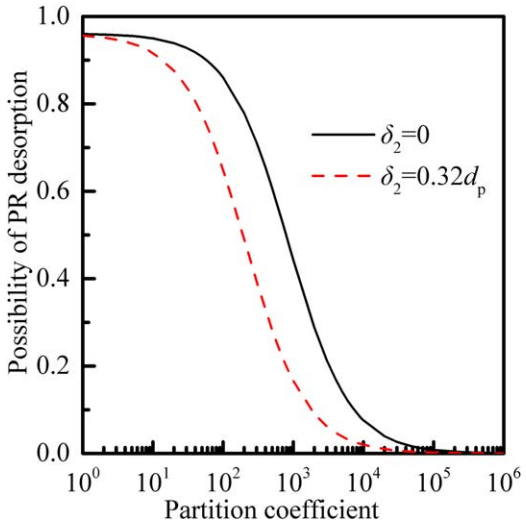

Figure 14. Theoretically predicted relationship between partition coefficient of PR (m_{PR}) and the possibility of PR desorption (P_d) at $\delta_2 = 0$ and 0.32 d_p.

[Color figure can be viewed in the online issue, which is available at wileyonlinelibrary.com.]

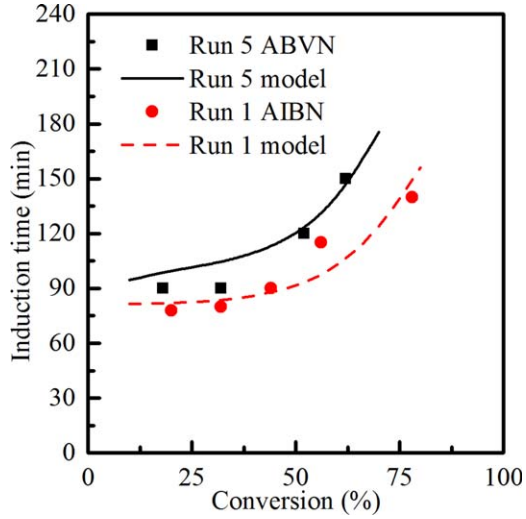

Figure 15. Comparison for the induction periods derived experimentally and predicted from model with AIBN and ABVN as initiator.

[Color figure can be viewed in the online issue, which is available at wileyonlinelibrary.com.]

PR desorption. The following parameters were used in the prediction: $D_p = 3.8 \times 10^{-7}$ dm^2/s, $D_{sl} = 1 \times 10^{-7}$ dm^2/s, $\delta_1 = 2$ nm, $D_w = 2.5 \times 10^{-7}$ dm^2/s, $\delta_2 = 0$ and $0.32d_p$, $m_{PR} = 1$–1×10^6, and $d_p = 85.0$ nm.

According to Eqs. 12 and 8, the effect of PR partition coefficient on the possibility of PR desorption is shown in Figure 14. At $\delta_2 = 0$, the possibility of desorption is about 95% when the partition coefficient of PR is used for prediction; while it decreases to about 85% when the partition coefficient of AIBN is used. At $\delta_2 = 0.32d_p$, the relative possibilities of desorption become 91 and 62%, respectively. Small partition coefficient means that the driving force of desorption is large. Therefore, the mass-transfer resistance changes to the stagnant aqueous film and the desorption becomes sensitive to the property of stagnant aqueous film. In this case, the effect of stagnant aqueous film thickness could not be ignored.

The polymerization rate predicted from PR partition is higher than that predicted from the AIBN partition, demonstrating that the PR desorption is a critical factor influencing the polymerization rate.[27] When the "absolute" oil-soluble initiators such as lauryl peroxide are used, the partition coefficient is large. In this case, the possibility of PR desorption is extremely low and the effective radicals for polymerization are few, leading to the low value of $\bar{n}$.[40]

ABVN was selected as another oil-soluble initiator to compare with AIBN. The 2-cynao-2-isoheptyl radical formed from ABVN was more hydrophobic than the 2-cynao-2-proply radical formed from AIBN.[41] The formation rates of radicals for the ABVN and AIBN systems were controlled to be the same in the prepolymerization step (Supporting Information). The results are shown in Figures 15. When the ABVN was used as the initiator, the model predictions agree well with the experiment results, although the parameters of 2-cynao-2-proply radical were used instead of those for the 2-cynao-2-isoheptyl radical in modeling. The solubility of 2-cynao-2-isohepty radical is smaller than that of 2-cynao-2-propyl radical. Meanwhile, the 2-cynao-2-isoheptyl radical has longer carbon chain than the 2-cynao-2-propyl radical, and the Flory–Huggins interaction parameter is of the former is larger.[42] The partition coefficient, which is the product of the water solubility and the exponent of Flory–Huggins interaction parameter,[27] does not change much. Therefore, the good predictions were obtained when the partition coefficient of 2-cynao-2-propyl radical was used for the ABVN system.

Conclusions

A model describing the PR desorption from the particle to aqueous phase in the traditional miniemulsion polymerization is established to predict the possibility of PR desorption when oil-soluble initiator is used. Experiment methods were also proposed to evaluate the PR desorption rate directly. The model predictions agree well with the experiment results. It is found that the possibility of PR desorption becomes low with the increase of diffusion resistance. Experiment results and model predictions indicate that PR is prone to desorb from the particle into the aqueous phase. PR desorption–reabsorption is a critical process to produce the effective radicals in the miniemulsion polymerization initiated by oil-soluble initiator. The theoretical model proposed herein will be helpful to understand the miniemulsion polymerization kinetics with oil-soluble initiators and other kinds of polymerization process in which the radical desorption involved.

Notation

List of parameters for prediction

D_p = diffusion coefficient of PR in the particle, 3.8×10^{-7} dm^2/s (Appendices A and B)

D_{sl} = diffusion coefficient of PR in the surfactant layer, 1×10^{-7} dm^2/s for SDS, 7.2×10^{-9} dm^2/s for Tween-20[39]

D_w = diffusion coefficient of PR in the aqueous phase (stagnant aqueous film), 2.5×10^{-7} dm^2/s (Appendix A)

m_{PR} = partition coefficient of PR between the organic (particle and droplet) and aqueous phase, 4.34–10.98[27]

δ_1 = thickness of the surfactant layer, 2×10^{-8} dm for SDS, 3.3×10^{-8} dm for Tween-20[37,38]

δ_2 = thickness of the stagnant aqueous film, 0–0.32d_p
f = initiation efficiency, 0.6 for AIBN,[43] 0.75 for ABVN (Supporting Information), 0.6 for AIBA
k_d = decomposition rate coefficient of the initiator, 1.27×10^{-5}/s for AIBN, 7.44×10^{-5}/s for ABVN, 3.70×10^{-5}/s for AIBA[43,44]
k_{dFS} = decomposition rate coefficient of FS, 1.57×10^{-4}/s
k_{pPR} = propagation rate coefficient between PR and monomer, 4.05×10^3 L/mol s[45,46]
k_{tPR} = termination rate coefficient between two PRs, 2×10^9 L/mol s[26]
k_{tFS} = termination rate coefficient between PR and FS, 2×10^9 L/mol s[34,35]
N_A = Avogadro's constant, 6.02×10^{23}/mol
ψ_B = "association parameter" for the solvent, 1 for St, 2.6 for water[47]
M_B = molecule weight of Solvent B, 18 g/mol for water, 104 g/mol for St
T = reaction temperature, 333.15 K
μ = viscosity of solvent, 0.4665 mPa s for water, 0.4503 mPa s for St[48]
V_A = molar volume of the Solute A as liquid at its normal boiling point, 88.37 cm^3/mol[48]

Acknowledgment

The authors thank the financial supports from the Innovation Research Team of Zhejiang Province (2009R50016), the National Natural Science Foundation of China (No. 21176210), the New Century Excellent Talent Project of Education Ministry (NCET-05-0512) and Outstanding Youth Foundation of Zhejiang Province (R4110199).

Literature Cited

1. Tiarks F, Landfester K, Antonietti M. Preparation of polymeric nanocapsules by miniemulsion polymerization. *Langmuir*. 2001;17:908–918.
2. Cao ZH, Shan GR. Synthesis of polymeric nanocapsules with a crosslinked shell through interfacial miniemulsion polymerization. *J Polym Sci Part A: Polym Chem*. 2009;47:1522–1534.
3. Ni KF, Shan GR, Weng ZX, Sheibat-Othman N, Fevotte G, Lefebvre F, Bourgeat-Lami E. Synthesis of hybrid core-shell nanoparticles by emulsion (co)polymerization of styrene and gamma-methacryloxypropyltrimethoxysilane. *Macromolecules*. 2005;38:7321–7329.
4. Zhang SW, Zhou SX, Weng YM, Wu LM. Synthesis of silanol-functionalized latex nanoparticles through miniemulsion copolymerization of styrene and gamma-methacryloxypropyltrimethoxysilane. *Langmuir*. 2006;22:4674–4679.
5. Cao ZH, Shan GR, Fevotte G, Sheibat-Othman N, Bourgeat-Lami E. Miniemulsion copolymerization of styrene and gamma-methacryloxypropyltrimethoxysilane: kinetics and mechanism. *Macromolecules*. 2008;41:5166–5173.
6. Cao ZH, Landfester K, Ziener U. Preparation of dually, pH- and thermo-responsive nanocapsules in inverse miniemulsion. *Langmuir*. 2012;28:1163–1168.
7. van Zyl AJP, Bosch RFP, McLeary JB, Sanderson RD, Klumperman B. Synthesis of styrene based liquid-filled polymeric nanocapsules by the use of RAFT-mediated polymerization in miniemulsion. *Polymer*. 2005;46:3607–3615.
8. Maxwell IA, Morrison BR, Napper DH, Gilbert RG. Entry of free radicals into latex particles in emulsion polymerization. *Macromolecules*. 1991;24:1629–1640.
9. Smith WV, Ewart RH. Kinetics of emulsion polymerization. *J Chem Phys*. 1948;16:592–599.
10. Nomura M, Ikoma J, Fujita K. Kinetics and mechanisms of particle formation and growth in the emulsion polymerization initiated by the oil-soluble initiator, 2,2'-azobisisobutyronitrile. *ACS Symp Ser*. 1992;492:55–71.
11. Nomura M, Ikoma J, Fujita K. Kinetics and mechanisms of emulsion polymerization initiated by oil-soluble initiators. 4. Kinetic modeling of unseeded emulsion polymerization of styrene initiated by 2,2′-azobisisobutyronitrile. *J Polym Sci Part A: Polym Chem*. 1993;31:2103–2113.
12. Mørk PC, Makame Y. Compartmentalized polymerization with oil-soluble initiators. Kinetic effect of single radical formation. *J Polym Sci Part A: Polym Chem*. 1997;35:2347–2354.
13. Asua JM, Rodriguez VS, Sudol ED, El-Aasser MS. The free-radical distribution in emulsion polymerization using oil-soluble initiators. *J Polym Sci Part A: Polym Chem*. 1989;27:3569–3587.
14. Suzuki K, Goto A, Takayama M, Muramatsu A, Nomura M. An experimental study on the kinetics and mechanisms of styrene polymerization in oil-in-water microemulsion initiated by oil-soluble initiators. *Macromol Symp*. 2000;155:199–212.
15. Alduncin JA, Forcada J, Barandiaran MJ, Asua JM. On the main locus of radical formation in emulsion polymerization initiated by oil-soluble initiators. *J Polym Sci Part A: Polym Chem*. 1991;29:1265–1270.
16. Blythe PJ, Klein A, Phillips JA, Sudol ED, El-Aasser MS. Miniemulsion polymerization of styrene using the oil-soluble initiator AMBN. *J Polym Sci Part A: Polym Chem*. 1999;37:4449–4457.
17. Brooks BW, Makanjuola BO. Measurements of the rate of radical desorption from polymer lattices during emulsion polymerization. *J Chem Soc Faraday Trans I*. 1981;77:2659–2667.
18. Chern CS. Desorption of free-radicals in semibatch emulsion polymerization of methyl acrylate. *J Appl Polym Sci*. 1995;56:231–238.
19. Brooks BW. Radical desorption in the emulsion polymerisation of vinyl monomers. *Colloid Polym Sci*. 1987;258:58–64.
20. Nomura M, Harada M. Rate coefficient for radical desorption in emulsion polymerization. *J Appl Polym Sci*. 1981;26:17–26.
21. Asua JM, Sudol ED, Elaasser MS. Radical desorption in emulsion polymerization. *J Polym Sci Part A: Polym Chem*. 1989;27:3903–3913.
22. Fellows CM, Murison RD, Russell GT. Model discrimination of radical desorption kinetics in emulsion polymerisation. *Macromol Theory Simul*. 2011;20:425–432.
23. Asua JM. A new model for radical desorption in emulsion polymerization. *Macromolecules*. 2003;36:6245–6251.
24. Casey BS, Morrison BR, Maxwell IA, Gilbert RG, Napper DH. Free-radical exit in emulsion polymerization. 1. Theoretical model. *J Polym Sci Part A: Polym Chem*. 1994;32:605–630.
25. Morrison BR, Casey BS, Lacik I, Leslie GL, Sangster DF, Gilbert RG, Napper DH. Free-radical exit in emulsion polymerization. 2. Model discrimination via experiment. *J Polym Sci Part A: Polym Chem*. 1994;32:631–649.
26. Autran C, de la Cal JC, Asua JM. (Mini)emulsion polymerization kinetics using oil-soluble initiators. *Macromolecules*. 2007;40:6233–6238.
27. Shang Y, Shan GR. IBN partition between St monomer/polymer and water and its application in miniemulsion polymerization initiated by AIBN. *AIChE J*. 2012;58:3135–3143.
28. Hernandez HF, Tauer K. Radical desorption kinetics in emulsion polymerization. 1. Theory and simulation. *Ind Eng Chem Res*. 2008;47:9795–9811.
29. Hernandez HF, Tauer K. Radical desorption kinetics in emulsion polymerization. 2. Brownian dynamics simulation of radical desorption in non-homogeneous particles. *Macromol Theory Simul*. 2010;19:249–257.
30. Einstein A. Zur Theorie der brownschen bewegung. *Ann Phys*. 1906;324:371–381.
31. Zimmer H, Lankin DC, Horgan SW. Oxidations with potassium nitrosodisulfonate (Fremy's Radical). *The Teuber reaction. Chem Rev*. 1971;71:229–246.
32. Lacik I, Casey BS, Sangster DF, Gilbert RG, Napper DH. Desorbed free-radicals in emulsion polymerizations: effect of aqueous-phase spin trap. *Macromolecules*. 1992;25:4065–4072.
33. Wilson BJ, Hayes JM, Durbin JA. Decomposition of nitrosyldisulfonate free-radical anion in non-aqueous solvents. *Inorg Chem*. 1976;15:1702–1704.
34. Bowry VW, Ingold KU. Kinetics of nitroxide radical trapping. *2. Structural effects. J Am Chem Soc*. 1992;114:4992–4996.
35. Beckwith ALJ, Bowry VW, Ingold KU. Kinetics of nitroxide radical trapping. *1. Solvent effects. J Am Chem Soc*. 1992;114:4983–4992.
36. Wilson BJ, Ritter DM. Decomposition of nitrosyl disulfonate ion in mildly alkaline solution. *Inorg Chem*. 1963;2:974–978.
37. Berr SS, Jones RRM. Effect of added sodium and lithium chlorides on intermicellar interactions and micellar size of aqueous dodecylsulfate aggregates as determined by small-angle neutron-scattering. *Langmuir*. 1988;4:1247–1251.
38. Khlebtsov BN, Chumakov EM, Semyonov SV, Chumakov MI, Khlebtsov NG. Study of complex micellar systems by static and dynamic light scattering. *2003 Saratov Fall Meeting: Coherent Optics of Ordered and Random Media IV, Saratov, Russia. Vol. 5475:12-20*. Bellingham: SPIE-International Society for Optical Engineering, 2004.
39. Yamane Y, Ando I, Buchholz FL, Reinhardt AR, Schlick S. Detection of spatial inhomogeneity in poly(acrylic acid) gels by measuring time-dependent diffusion coefficients of a probe in NMR

experiments: effect of the degree of cross-linking and degree of swelling. *Macromolecules*. 2004;37:9841–9849.
40. Alduncin JA, Forcada J, Asua JM. Miniemulsion polymerization using oil-soluble initiators. *Macromolecules*. 1994;27:2256–2261.
41. Stephenson RM. Mutual solubility of water and nitriles. *J Chem Eng Data*. 1994;39:225–227.
42. Bernardo G, Vesely D. Solubility of alkanes in a polystyrene matrix. *J Appl Polym Sci*. 2008;110:2393–2398.
43. Rawlston JA, Guo J, Schork FJ, Grover MA. A kinetic Monte Carlo study on the nucleation mechanisms of oil-soluble initiators in the miniemulsion polymerization of styrene. *J Polym Sci Part A: Polym Chem*. 2008;46:6114–6128.
44. Brandrup J, Immergut EH, Grulke EA, Abe A, Bloch DR. *Polymer Handbook*, *4th ed*. New York: Wiley, 1999.
45. Fischer H, Radom L. Factors controlling the addition of carbon-centered radicals to alkenes-an experimental and theoretical perspective. *Angew Chem Int Ed*. 2001;40:1340–1371.
46. Heberger K, Fischer H. Rate constants for the addition of the 2-cyano-2-propyl radical to alkenes in solution. *Int J Chem Kinet*. 1993;25:249–263.
47. Bird RB, Stewart WE, Lightfoot EN. *Transport Phenomena*, *2nd ed*. New York: Wiley, 2001.
48. Lide DR. *CRC Handbook of Chemistry and Physics*, *85th ed*. Boca Raton: CRC Press, 2003.
49. Friis N, Hamielec AE. Gel-effect in emulsion polymerization of vinyl monomers. *ACS Symp Ser*. 1976;24:82–91.
50. Sundberg DC, Hsieh JY, Soh SK, Aldus RFB. Diffusion-controlled kinetics in the emulsion polymerization of styrene and methyl methacrylate. *ACS Symp Ser*. 1981;165:327–343.

Appendix A

The diffusion coefficient of PR in St and water is estimated by Wilke–Chang equation[47]

$$D_{AB} = 7.4\times10^{-10}\frac{\sqrt{\psi_B M_B}T}{\mu V_A{}^{0.6}}\left(\mathrm{dm}^2/\mathrm{s}\right) \tag{A1}$$

Equation A1 describes the diffusivity for low concentrations of A in Solvent B. Isobutyronitrile is selected as the substitute of 2-cynao-2-propyl radical to estimate the diffusion coefficient.

Appendix B

k_{tPR}, [M], and D_p are all related to the conversion of polymerization. k_{tPR} is mainly affected by gel effect. The ratio of k_{tPR} to its initial value (k_{tPR0}) at conversion zero could be express as[49]

$$\begin{gathered} k_{tPR}/k_{tPR0} = \exp\left(-2(Bx+Cx^2+Dx^3)\right) \\ B = 2.57-5.05\times10^{-3}T \\ C = 9.56-1.76\times10^{-2}T \\ D = -3.03-7.85\times10^{-3}T \end{gathered} \tag{B1}$$

The ratio of D_p to its initial value (D_{p0}) in the particle is related as[50]

$$k_{tPR}/k_{tPR0} = D_p/D_{p0} \tag{B2}$$

Appendix C

Assuming that the polymer particle is surrounded by part of the water, it can form a "water ball" with the polymer particle as core. These "water balls" are supposed to be in the close-packing form. Therefore, the volume fraction of "water balls" is $\frac{\pi}{3\sqrt{2}}$ (74.1%) space in the miniemulsion. The other 25.9% (1–74.1%) is occupied by the water. The solid content is 15% in the miniemulsion polymerization. On the basis of density values of water and St at 60°C, the volume fraction of polymer particle is estimated to be 16.6% in the miniemulsion. The volume ratio of the polymer particle core to the "water ball" is 16.6 : 74.1=0.224 : 1. Therefore, the diameter ratio of the polymer particle core to the "water ball" is $\sqrt[3]{0.224:1}$=0.607 : 1. The average distance between each particle center equals to $1.65d_p$ $\left(\frac{1}{0.607}=1.65\right)$.

Manuscript received Aug. 12, 2013, and revision received Apr. 28, 2014.